1253463

THE UNITED STATES OF AMERICA

TO ALL TO WHOM THESE PRESENTS SHALL COME:

UNITED STATES DEPARTMENT OF COMMERCE

United States Patent and Trademark Office

November 26, 2004

THIS IS TO CERTIFY THAT ANNEXED HERETO IS A TRUE COPY FROM THE RECORDS OF THE UNITED STATES PATENT AND TRADEMARK OFFICE OF THOSE PAPERS OF THE BELOW IDENTIFIED PATENT APPLICATION THAT MET THE REQUIREMENTS TO BE GRANTED A FILING DATE.

APPLICATION NUMBER: *60/494,358*
FILING DATE: *August 12, 2003*
RELATED PCT APPLICATION NUMBER: *PCT/US04/25373*

Certified by

Jon W Dudas

Acting Under Secretary of Commerce
for Intellectual Property
and Acting Director of the U.S.
Patent and Trademark Office

PROVISIONAL APPLICATION FOR PATENT COVER SHEET
This is a request for filing a PROVISIONAL APPLICATION FOR PATENT under 37 CFR 1.53(c).

Express Mail Label No.	

INVENTOR(S)

Given Name (first and middle [if any]	Family Name or Surname	Residence (City and either State or Foreign Country)
NATHAN	INTRATOR	PROVIDENCE RI

Additional inventors are being named on the _____ one _____ separately numbered sheets attached hereto

TITLE OF THE INVENTION (500 characters max)

Direct all correspondence to:	**CORRESPONDENCE ADDRESS**
☐ Customer Number:	
OR	
☑ Firm or Individual Name	
Address	Box 2605
Address	

City	PROVIDENCE	State	RI	Zip	02906
Country	USA	Telephone	401 837 0351	Fax	401 633 6016

ENCLOSED APPLICATION PARTS (check all that apply)

☑ Specification *Number of Pages* ___5___   ☐ CD(s), Number _____

☑ Drawing(s) *Number of Sheets* ___1___   ☑ Other (specify) _Attached I.P. paper_

☐ Application Date Sheet. See 37 CFR 1.76

METHOD OF PAYMENT OF FILING FEES FOR THIS PROVISIONAL APPLICATION FOR PATENT

☑ Applicant claims small entity status. See 37 CFR 1.27.

☑ A check or money order is enclosed to cover the filing fees.

☐ The Director is herby authorized to charge filing
fees or credit any overpayment to Deposit Account Number: _____

☐ Payment by credit card. Form PTO-2038 is attached.

FILING FEE
Amount ($)
75

The invention was made by an agency of the United States Government or under a contract with an agency of the United States Government.

☑ No.

☐ Yes, the name of the U.S. Government agency and the Government contract number are: _____

[Page 1 of 2]

Respectfully submitted,

SIGNATURE _____   Date __Aug 5, 03__

TYPED or PRINTED NAME __NATHAN INTRATOR__   REGISTRATION NO. _____
(if appropriate)

TELEPHONE __401 837 0351__   Docket Number: _____

USE ONLY FOR FILING A PROVISIONAL APPLICATION FOR PATENT

PROVISIONAL APPLICATION COVER SHEET
Additional Pag

Docket Number		

INVENTOR(S)/APPLICANT(S)		
Given Name (first and middle [if any]	Family or Surname	Residence (City and either State or Foreign Country)
Ki-o	Kim	Providence RI

[Page 2 of 2]

Number ___1___ of ___1___

Provisional Patent Application of

Nathan Intrator and Ki-o Kim

For

TITLE: IMPROVED ECHO DELAY ESTIMATES FROM MULTIPLE SONAR PINGS

CROSS-REFERENCE TO RELATED APPLICATIONS: None

SEQUENCE LISTING: None

BACKGROUND

Sonar echo delay estimation is affected by several factors: Sonar pulse strength, noise level, frequency range, medium dispersion properties and pulse shape and duration. Multiple sonar pings can reduce the sensitivity to noise and thus, improve echo delay estimation. This is done by taking the mean of the of the echo delay estimation from each ping. We disclose a method and apparatus for improving sonar echo delay estimation by using additional information that can be extracted from multiple sonar pings. General sonar prior art is reviewed in [1,2,3]. More recent work can be found in [6].

In current sonar methodology, the algorithm to analyze the returned sonar signal does not adapt to the level of SNR. There is work on adaptive beam forming and adaptive noise cancellation methods, but these depend on knowing something about the noise source, for example when the source of noise comes from the submarine itself. However, the current disclosure discusses adaptive changes to the preprocessed signal after beam forming and is independent of the beam forming. The disclosed method adapts to the noise by analyzing the effect of noise on the distribution of echo delay estimation. Adaptive noise-dependent sonar processing was described in [4,5,6]. There the information gathered from multiple pings was used to focus echo delay estimation on specific frequency bands that were better for delay estimation at those noise levels. The disclosed method can perform its calculation in the time domain only as well as in time/frequency domain. It relies on further analysis of the distribution of echo delay estimates from multiple pings and removing pings that fall outside of some defined distribution boundaries. Thus, the final, more accurate, echo delay estimation relies on those pings that fall within the distribution boundaries.

SUMMARY

A method and apparatus for obtaining and improving range estimation between successive signals or between the transmitted signal and an echo return is disclosed. The method includes a detailed estimation of the distribution of echo delays from the successive pings and elimination of pings which provide estimation that is outside of some boundaries of the distribution. The remaining pings are used for improved echo delay estimation.

DRAWINGS

FIG. 1 is a schematic diagram of the adaptive echo delay estimation

DESCRIPTION OF THE FIGURE

Figure 1 presents a schematic diagram of the algorithm. Multiple echoes 11, are preprocessed and analyzed. The distribution of echo delay estimation 12, is analyzed and a threshold is determined 13, to eliminate some echo returns 14, that are outside of the boundaries of the distribution. The mean of the remaining echoes 15, is found. The new mean is compared 16, to the mean that has been determined with no threshold or using previously determined threshold. If the new mean has changed (beyond a certain value), the loop continues so that the distribution of echo delays is further analyzed using the echoes that remain after the new threshold is applied 15, otherwise the loop stops 17, and the final mean is given as the echo delay estimation.

REFERENCE NEUMERALS

11 Multiple echoes are preprocessed and analyzed.

12 The distribution of echo delay estimation is analyzed.

13 A threshold of data elimination based on the distribution is determined.

14 Echo returns are eliminated if they are outside of the boundaries of the distribution.

15 The mean of the remaining echoes is found.

16 The new mean is compared to the mean that was determined with no threshold or using previously determined threshold.

17 If the mean has changed (beyond a certain value) the loop continues, otherwise the loop stops and the final mean is given as the echo delay estimation.

OPERATION

The operation of the echo delay distribution estimation 12, 13, is described in detail in [7]. The determination of a threshold is based on determination of a number of standard deviations from the center of the distribution. It can also be based on deviations of a cycle width (given the highest frequency in the pinging signal.)

CLAIMS

1. A method and apparatus for estimation of echo delay measurements from multiple sonar returns comprising of:

    • Signal conditioning and noise cancellation to improve signal characteristics, based on known or unknown information about the nature of the noise and the characteristics of the transfer media.

    • A means to measure echo delay from successive pings.

    • Analysis of the distribution of echo delays from the multiplicity of pings.

    • Determination of a rule on which to reject ping returns which do not provide useful information about the echo delay.

    • Rejection of returned pings based on above rule.

    • Estimation of echo delay based on information from all the echo returns that were not rejected by the rejection algorithm.

2. A system as in claim 1 wherein the echo delay measurements is performed in the time domain. This can be done directly on the raw signal or on some transformations of the raw signal such as Hilbert transform, absolute value, string length etc.

3. A system as in claim 1 wherein the echo delay measurements is performed in the time/frequency domain.

4. A system as in claim 1 wherein the distribution of the echo delay estimation is created using multiple bandwidth analysis of the data as done in [4,5,6].

ABSTRACT

A method to improve sonar echo delay estimation from multiple sonar pings is disclosed. The method relies on multiple measurements and estimations of the echo delay distribution from raw or preprocessed signal.

REFERENCES

1. Baggeroer, A.B. Chapter 6 -Sonar Signal Processing Book title: Applications of Digital Signal Processing Editor: Oppenheim, A.V. Publisher: Englewood Cliffs, NJ, Prentice Hall, 1978 ISBN 0-13-039115-8

2. Bruce, M.P., A processing Requirement and Resolution Capability of Side-Scan and Synthetic aperture Sonars IEEE Journal of Oceanic Engineering, Vol 17, Number 1 (Special Issue), January 1992 pp 106-117

3. McHugh,R., Shaw,S., Taylor,N.T., Efficient digital signal processing algorithm for sonar imaging, IEE Proc.-Radar, Sonar Navig., Vol. 143, NO.3, June 1996.

4. Cooper L. N, Intrator N, Neretti N., Adaptive noise level estimation for sonar signal processing. Provisional Patent, Submitted, May 31, 2003.

5. Cooper L. N, Intrator N, Neretti N., Noise adaptive sonar signal processor. Provisional Patent, Submitted, May 31, 2003.

6. Neretti N, Intrator N, Cooper L. N. Adaptive pulse optimization for improved range accuracy. Submitted to IEEE Signal Processing Letters. May, 2003.

7. K. Kim, N. Intrator. Classification of Dolphin Clicks in Time Domain Representation.Preprint attached to the current PPA.

8. P. M. Woodward, *Probability and Information Theory, with Applications to Radar.* New York: McGraw-Hill Book Company, Inc., 1953.

9. N. Neretti, M. I. Sanderson, J. A. Simmons and N. Intrator, Time-frequency computational model for echo-delay resolution in sonar images of the big brown bat, Eptesicus fuscus. *Journal of the Acoustical Society of America 113 (4), pp. 2137-2145, April 2003.*

Classification of Dolphin Clicks in Time Domain Representation

Kio Kim
Nathan Intrator

Department of Physics, Brown University, Providence, Rhode Island, 02912

4 August 2003

1 Introduction

Dolphins and bats use sonar to locate and identify objects. Dolphins' emit acoustic signals from a fat-filled organ near the nasal cavity, while most mammals use larynx to make sound. The returning signal comes through their lower jaw, and finally reaches the middle ear [1, 2]. The acoustic signal is transformed into a neural signal at the basilar membrane, which stimulates inner hair cells of corresponding frequencies.

Roitblat *et al.* have let dolphins perform matching-to-sample tasks. They have recorded the signals generated by the dolphins and those reflected by the objects [3]. Matching-to-sample task amounts to classifying the returning signals. There has been some work in classifying the returning signals in [4, 5, 6], as well as the pinging signals [7, 8]. Moore *et al.* have filtered the recorded returning signals with 30 bandpass filters, and used the output to drive an artificial neural network for classification [4, 5]. Gaunaurd *et al.* have analyzed the dolphin returning signals, and extracted in a heuristic manner, information from the returning pings and their frequency representation. Based on the heuristic approach he then suggested an automated classification method using time-frequency analysis [6].

In this paper, we demonstrate a straight forward method for estimation of echo delays from multiple returning pings. We introduce a (iterative) algorithm to improve the estimation based on elimination of ping returns which were determined not to be informative to the ensemble. We further demonstrate that different methods for estimating the exact location of a wave front can have different types of errors and thus might be useful for discrimination of different objects. Finally, we show that a combination of these wave front estimation methods together with the improved echo delay estimation from multiple pings leads to very good results on the dolphin classification data.

2 Experimental Setup

A dolphin was trained to perform a matching-to-sample tasks. The dolphins? pinging signals as well as the returning signals from objects were recorded. The specific task of this bottlenose dolphin (*Tursiops truncatus*) was to identify the fluid which the submerged cylinders contained (Fig. 1). Target objects are containers filled with fresh or saline water, glycerol, or kerosene. Each trial

begins with a tone signaling at which dolphin voluntarily place his head in the observing aperture. One of sample objects is presented to the dolphin, and the dolphin examines the object with several pinging signals. After the dolphin stops pinging, the sample object is removed and three comparison objects are exposed to the dolphin. The dolphin tries to identify one target object which matches the sample object, and indicates his choice by moving one of three response wands which corresponds to the matching comparison object. The sample object and comparison objects are located 4.83m and 3.85m ahead from the observing aperture, respectively. The dolphin is rewarded by food when making the correct decision.

The dolphin's pinging and returning signals were recorded by hydrophones placed between the dolphin and target objects, and digitized at 512 kHz.

A total of 133 trials were recorded. These include 20 fresh water trials, 50 saline water, 34 glycerol, and 29 kerosene trials. Each trial contains up to 98 pairs of pinging and returning signal (due to a system limitation). A total of 8848 pairs were recorded; 1208 from fresh water, 3144 from saline water, 2705 from glycerol, and 1791 from kerosene..

2.1   Returning Signal Properties

The physical properties of kerosene and glycerol differ from each other, and from fresh or saline water. Due to the appreciable difference of the density and compressibility between kerosene, glycerol, and water, we can identify the liquid inside the target object based on the sound velocity in each liquid. The difference between Fresh and Saline water properties is much smaller, thus discrimination between targets that were filled with either type was more challenging. The dolphin pinging signal is broad band, and has a prominent peak in the time domain representation (Fig. 2(a)). When the pinging signal is projected into a cylindrical target object, this peak is maintained after being bounced from the front and the back of the target, so we can detect two main peaks in the returning signal, and measure the time difference between them.

The two peak arrival times are defined by

$$t_{max,a} = \arg\max y(t) \tag{1}$$
$$t_{max,b} = \arg\max y'(t) \tag{2}$$

where $y(t)$ and $y'(t)$ are the preprocessed returning signal, and $y(t)$ with the peak around $t_{max,a}$ removed. PATD is given by:

$$\Delta \equiv |t_{max,a} - t_{max,b}|. \tag{3}$$

2.2   Preprocessing Methods and The Peak Arrival Time Difference (PATD)

PATD measured directly from the raw signal can have some shortcomings. First, the signal is subjected to phase inversion when it is reflected by a lower density medium, such as when the pinging signal is reflected by kerosene. Second, the peak detection in the time domain is sensitive to noise. Third, the wave shape evolves as it propagates in time due to the dispersion. These factors contribute to the temporal location uncertainty of peaks.

We introduce three different preprocessing methods to make the detection of PATD more stable; (i) Peak loss by phase inversion can be prevented by taking the absolute value of the returning signal:

$$y_a(t) = |x(t)|.$$

2

OVERHEAD
MONOFILAMENT
LINES

RESPONSE
WANDS

OBSERVING
APERTURE   ACOUSTIC
            SHUTTER   HYDROPHONES
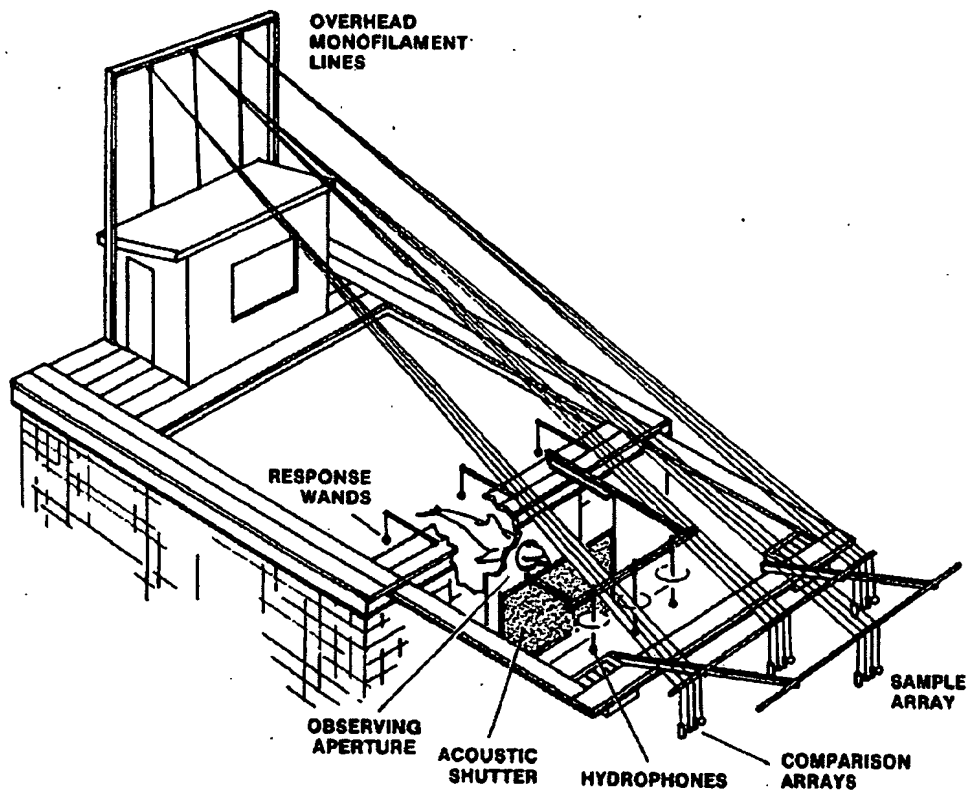
SAMPLE
ARRAY

COMPARISON
ARRAYS

Figure 1: Experimental setup for dolphin training and testing. Each trial begins with a tone signaling at which dolphin voluntarily place his head in the observing aperture. One of sample objects is presented to the dolphin, and the dolphin examines the object with several pinging signals. After the dolphin stops pinging, the sample object is removed and three comparison objects are exposed to the dolphin. The dolphin attempts to identify which matches the sample object, and indicates his choice by moving one of three response wands which correspond to three comparison objects.
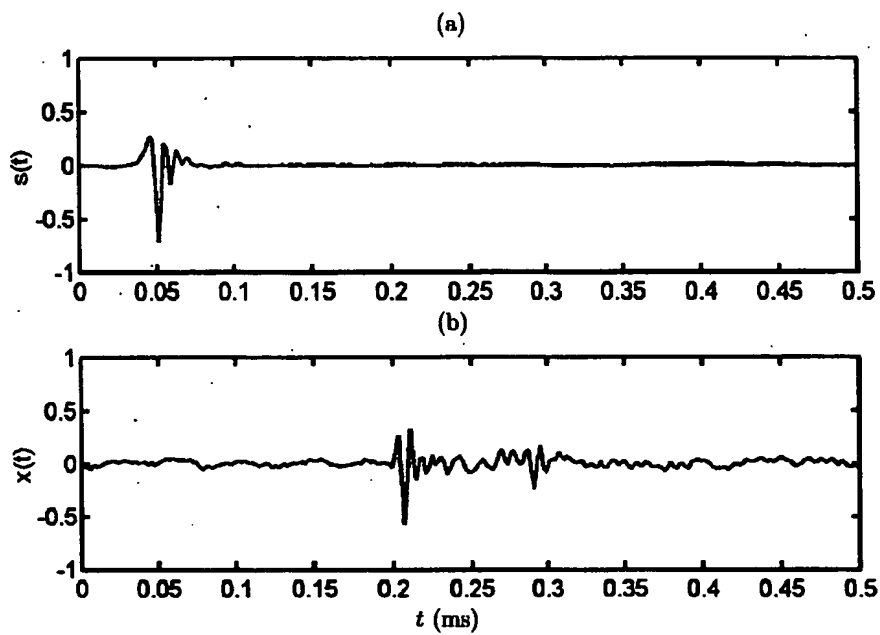
3

Figure 2: Waveform of a typical pinging and returning signal pair. (a) Waveform of a pinging signal. (b) Waveform of a returning signal of (a) after being reflected by a cylinder filled with fresh water.

4

(ii) The matched filter is a linear filter used to enhance detectability of the signal receiver by increasing the signal-to-noise ratio (SNR). The transfer function that yields the maximum SNR is the reverse of pinging signal itself, and the resulting output signal is,

$$y_m(t) = \int_{-\infty}^{\infty} x(t')s\big(-(t-t')\big)dt' = \int_{-\infty}^{\infty} x(t')s(t'-t)dt' = x(t) \star s(t),$$

where $s(t)$, and $x(t)$ are pinging and returning signals, respectively. [9]. (iii) In order to reduce the uncertainty caused by the time evolution of the wave shape, we can detect the peak of the wave envelope instead of the wave amplitude peak. This can be done with the instantaneous envelope which is the amplitude of an analytic signal, of which the real part is the recorded signal, and the imaginary part is the Hilbert transform of the signal [10]. The Hilbert transform, $\hat{x}(t)$, of a signal, $x(t)$ is obtained by convolving $x(t)$ with $\frac{1}{\pi t}$, which is,

$$\hat{x}(t) = x(t) \star \frac{1}{\pi t} = \frac{1}{\pi} \int_{-\infty}^{\infty} \frac{x(t')}{t-t'}dt', \tag{4}$$

or in the frequency domain,

$$\hat{X}(f) = -i\,\mathrm{sgn}(f)X(f), \tag{5}$$

where $\hat{X}(f)$ and $X(f)$ are Fourier transforms of $\hat{x}(t)$ and $x(t)$, respectively [11]. Thus, the envelope function $y_e(t)$ is,

$$y_e(t) = |x(t) + i\hat{x}(t)|.$$

In Fig. 3(a)∼(c), the results of three preprocessing methods applied to the signal in Fig. 2 are depicted, with the raw signal overlaid in scale by dotted line.

2.3 High Energy Criteria

We estimates the mean energy of both pinging and returning signals, and the mean wave envelope width of returning signals. Plotting them in (returning signal energy)$^{1/2}$ vs. (returning signal envelope width) and (returning signal energy)$^{1/2}$ vs. (pinging signal energy)$^{1/2}$ scatter plots, we have noticed that erroneous pinging and returning signal pairs are making separable clusters in those scatter plots. (See red dots in Fig. 4(a)∼(b) enclosed by dotted lines.)

Among 8848 pairs of signals, 926 pairs of signals are eliminated based on the energy of pinging and returning signals, and the ratio of returning signal energy and the root-mean-square width of returning signal envelope. We have validated that the eliminated signals lack clear peaks, and their wave shapes were different from those of normal ping and returning signals. After elimination, 7922 signal pairs remain; 965 fresh water pairs, 2796 of saline water, 2502 of glycerol, and 1659 of kerosene.

2.4 Mean PATD and Modified Mean PATD

The central limit theorem implies that the separability between different classes can be improved by taking the average of PATD's. Since a dolphin emits several pinging signals in each trial, we take the average of PATD's in a trial. However, due to various reasons related to the recording and triggering system, there are several recordings with lower signal-to-noise ratio or with no signal at all. Furthermore, as there was noise present during the recording process, there were returns where

5

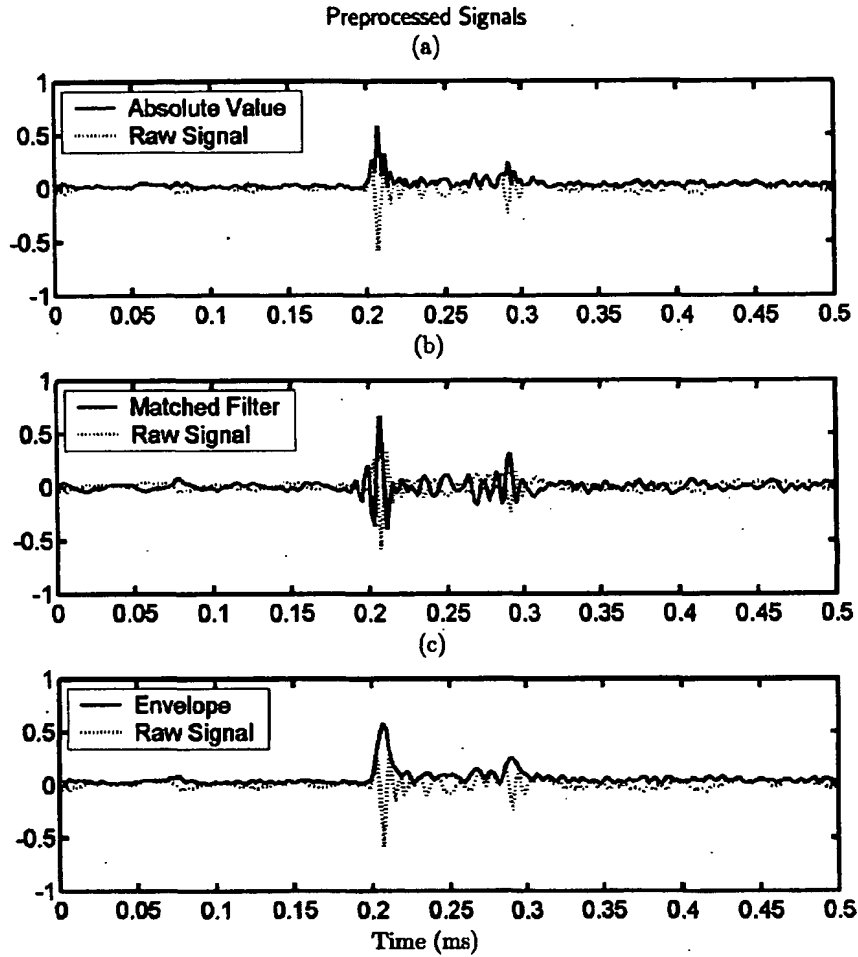Preprocessed Signals
(a)

(b)

(c)

Time (ms)

Figure 3: Dolphin pinging signal have a major peak in the time domain representation. The Peak Arrival Time Difference (PATD) is the arrival time difference between first and second peaks in the returning signal, which are peaks of the pinging signal reflected by the front and the back of the target object. For PATD detection, the returning signal has been processed by three different preprocessing methods: (a) Absolute value. (b) Matched filtering. Matched filter is the optimal linear filter that maximizes the signal-to-noise ratio (SNR) of returning signal. Matched filtering is mathematically equivalent to cross-correlating the returning signal with the pinging signal. Since the phase information is kept, the uncertainty is half the period. (c) Instantaneous envelope detection (IED). The shape of the envelope hardly changes, meanwhile the wave shape changes during the wave propagation. Thus, PATD detected from the envelope shape can be a more stable estimator. The instantaneous envelope is the magnitude of an analytic signal, of which the real part is the recorded signal, and the imaginary part is the Hilbert transform of the recorded signal.
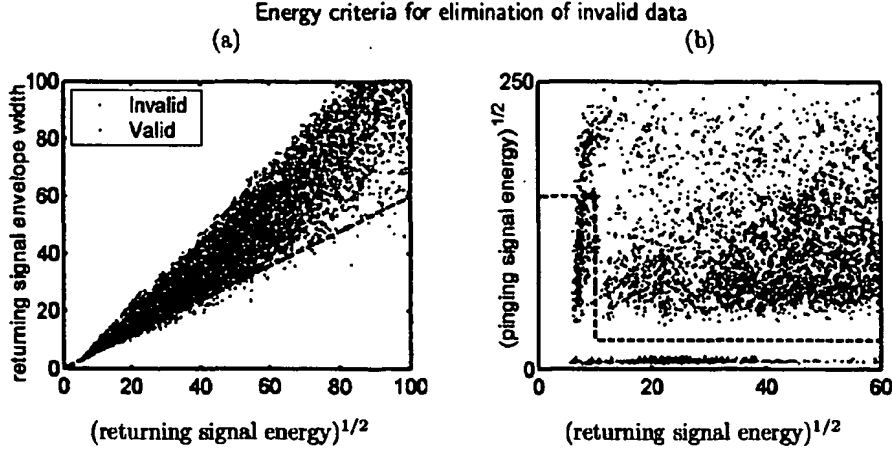
6

Energy criteria for elimination of invalid data

Figure 4: Erroneous pinging and returning signal pairs appear to be making separable clusters in scatter plots of (returning signal energy)$^{1/2}$ vs. (returning signal envelope width), and (returning signal energy)$^{1/2}$ vs. (pinging signal energy)$^{1/2}$. Invalid signal pairs are marked by red dots in two scatter plots. (a) (returning signal energy)$^{1/2}$ vs. (returning signal envelope width). (b) (returning signal energy)$^{1/2}$ vs. (pinging signal energy)$^{1/2}$.

the estimation of the peak of a wavefront was not detected correctly, as additive noise increase the amplitude of a neighboring cycle. The Modified Mean PATD is aimed at addressing these problems. We study the distribution of the echo delay estimation and define a threshold so that echo delays that are outside the boundaries of the distribution were not included in the modified calculation of the mean (see Fig. 5.) Thus, the Mean PATD (MPATD) of a trial is defined by the mean value of PATD's of the trial which are within the acceptance range. Since the recorded signals are digitized at 512 kHz of sampling frequency, PATD(Δ) is a discrete random variable, of which allowed values are 0.002, 0.004, $\cdots$, 0.498, 0.5 ms. We define a cluster by a group of PATD's of which bins are consecutively connected by bins with two or more PATD's. The mode cluster is the largest cluster in a trial, and the mode cluster range is the range of PATD's in the mode cluster. (See Fig. 5.) The mean value of PATD's within the mode cluster range is the Modified Mean PATD (MMPATD), $\bar{\Delta}'$.

3 Results

3.1 Signal-based classification

7922 returning signals were examined. The probability mass functions of PATD's of each class, $f_{fre}(\Delta)$, $f_{sal}(\Delta)$, $f_{gly}(\Delta)$, and $f_{ker}(\Delta)$ are estimated by normalizing the PATD histogram of each class (Fig. 6(a)). Curves were added by cubic spline interpolation.

Fig. 6(a), (b), and (c) present the probability mass functions of Δ_a, Δ_m, and Δ_e, respectively. The probability distribution of kerosene shows two peaks next to each other in Fig. 6(a). This is due to the absolute value operation, which have discarded the phase information, so that peaks

7

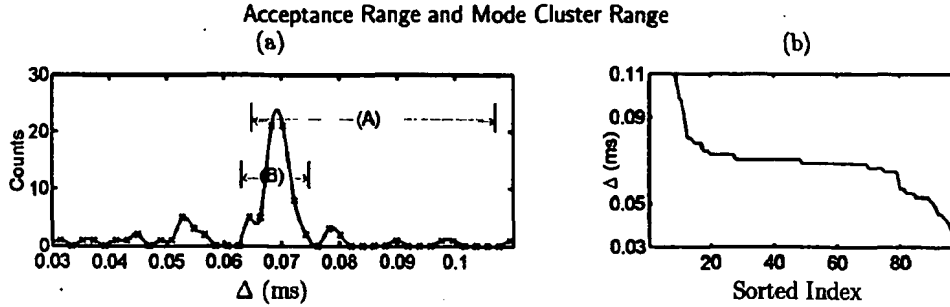Acceptance Range and Mode Cluster Range

Figure 5: (a) (A) and (B) represent the acceptance range and the mode cluster range of one of kerosene trial, respectively. The acceptance range is the smallest range which encloses the major PATD distribution peaks of four classes. The mode cluster range is the range of PATD's in the mode cluster, where the mode cluster is the largest cluster, and a cluster is a group of PATD's of which bins are consecutively connected by bins of two or more PATD's. The acceptance range is a fixed range throughout the trials, while the mode cluster range varies depending on trial. (b) PATD's in the same trial is displayed in descending order. It is clearly seen that there is a group of most frequently observed value of PATD's. The mode cluster range can assort PATD's in this group. For both (a) and (b), PATD's are from the first trial of kerosene class.

include both positive and negative peaks.

The probability distribution of saline PATD has shown periodic appearance of peaks. (Fig. 6(b).) It is attributed to the coherence of sound wave between the first and the second peaks. From inspection of pinging signals, the carrier period is 0.008ms, and the average PATD is 0.080 ms, which is an even number multiple of the carrier period. This coherence produces resonant standing wave inside the cylindrical target object filled with saline water. The matched filter reinforces the carrier frequency, so the resonance is clarified after matched filtering. (See Fig. 7.)

Fig. 6(c) indicates that the PATD measured from the wave envelope is stable and regular.

The PATD separability of three different preprocessing methods are tested by the classification of PATD using the maximum likelihood rule. The classification result of each signal is shown in Fig. 8, and the overall numerical performance is presented 1.

	Fre	Sal	Gly	Ker	Total
Δ_a	70.6%	37.3%	90.0%	82.4%	67.4%
Δ_m	61.6%	57.9%	85.5%	76.9%	71.1%
Δ_e	53.5%	54.3%	91.2%	85.4%	72.4%

Table 1: Percentages of returning signals correctly classified by the maximum likelihood rule applied to PATD's are presented. Δ_a, Δ_m, and Δ_e denote PATD's calculated after the absolute value operation, the matched filtering, and the instantaneous envelope detection. Fre, Sal, Gly, and Ker represent fresh water, saline water, glycerol, and kerosene, respectively. Percentages are calculated from the number of returning signals qualified by the high energy criterion, which are 965 of fresh water, 2796 of saline water, 2502 of glycerol, and 1659 of kerosene.
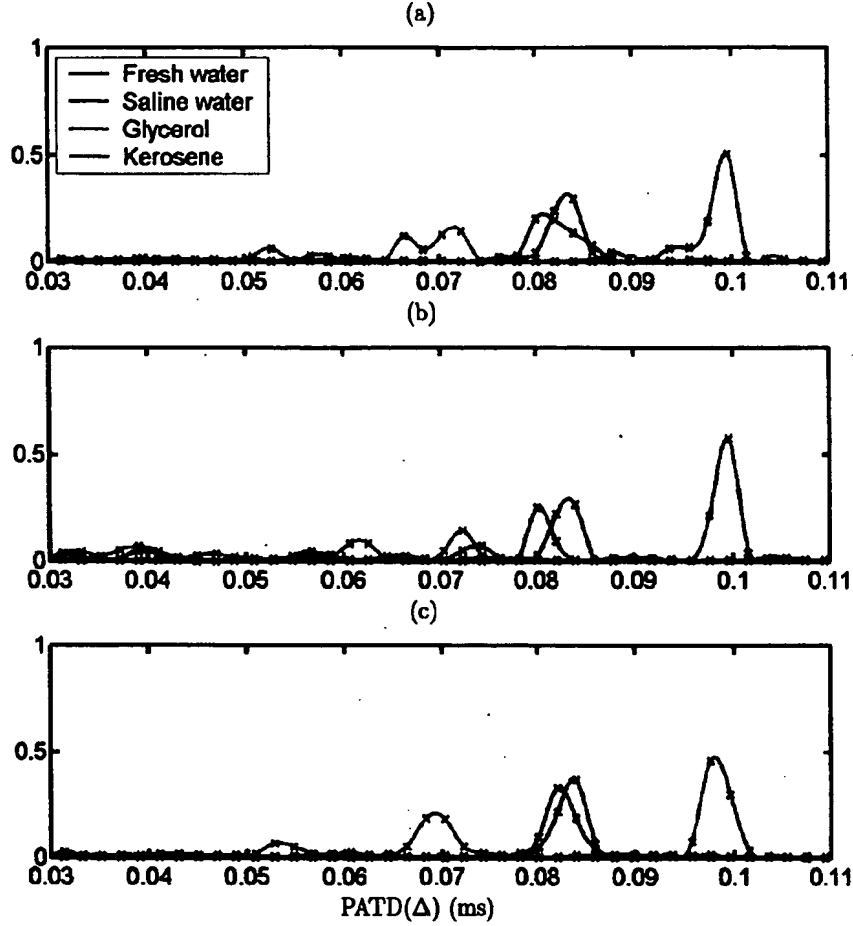
8

Figure 6: The probability mass functions (PMFs) of PATD's calculated after signals being processed in three different ways. PATD's of fresh water, saline water, glycerol, kerosene trials are represented by curves in blue, red, magenta, and cyan, respectively. (a) Absolute value. (b) Matched filtering. (c) Instantaneous envelope detection.
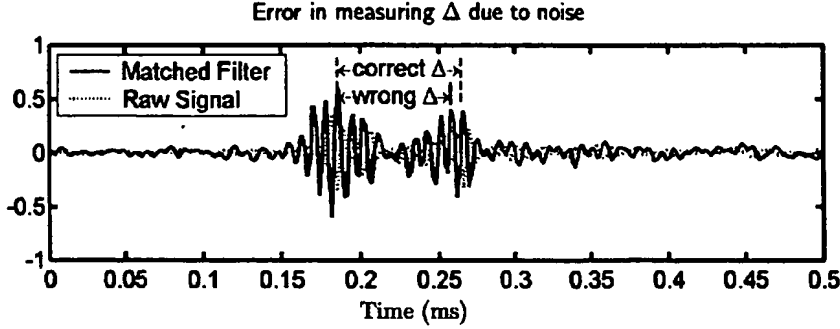
Error in measuring Δ due to noise

Figure 7: Many factors can give rise to a wrong second peak. Cross-correlating the returning signal with the pinging signal emphasizes the wavelike property of the returning signal. Additive noise, back scattering or other factors can change the amplitude of peaks in the cross-correlation. It can cause a wrong identification of the first and second peak detection and lead to error in the measurement of Δ by one period or more.

3.2 Trial-based Classification

The probability mass functions of MPATD and MMAPTD are depicted in Fig. 9 and Fig. 10. MMPATD shows better separation between classes than MPATD. Also, the excellency of MMPATD is quantitatively verified in Table 2 where the classification performance of MPATD and MMPATD are listed by preprocessing methods and target objects, and in Fig. 11(a)~(c). Note that $\bar{\Delta}'_a$ and $\bar{\Delta}'_e$ are good discriminants for separation of glycerol and kerosene classes, while $\bar{\Delta}'_m$ classifies fresh and saline water classes best. Actually, PMF peaks of $\bar{\Delta}'_m$ of fresh and saline water are completely separated in Fig. 10 (b). Also, $\bar{\Delta}'_e$ excels other estimates on the whole.

The classification was tested using k-nearest neighbor method with $k = 5$. There are 133 available trials, and classification was performed for each trial using the rest 132 trials as training data.

|	Fre	Sal	Gly	Ker	Total
$\bar{\Delta}_a$	5.0%	40.0%	82.4%	24.1%	42.1%
$\bar{\Delta}_m$	0.0%	58.0%	91.2%	31.0%	51.9%
$\bar{\Delta}_e$	0.0%	54.0%	82.4%	48.3%	51.9%
$\bar{\Delta}'_a$	5.0%	82.0%	100.0%	100.0%	78.9%
$\bar{\Delta}'_m$	80.0%	80.0%	100.0%	75.9%	84.2%
$\bar{\Delta}'_e$	60.0%	82.0%	100.0%	100.0%	87.2%

Table 2: Percentages of trials correctly classified by k-nearest neighbor method applied to MPATD and MMPATD. $\bar{\Delta}_a$, $\bar{\Delta}_m$, and $\bar{\Delta}_e$ represent MPATD calculated after the absolute value operation, the matched filtering, and the instantaneous envelope detection, and primed $\bar{\Delta}$'s denote MMPATD. Percentages are calculated from the number of trials, which are 20 of fresh water, 50 of saline water, 34 of glycerol, and 29 of kerosene.
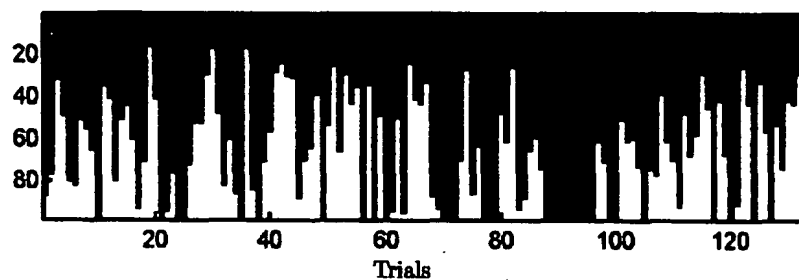
10
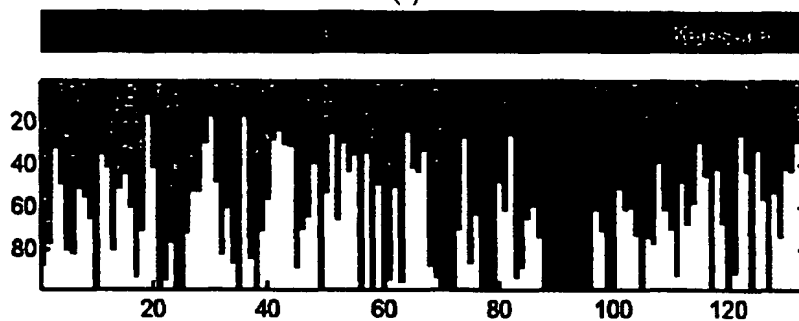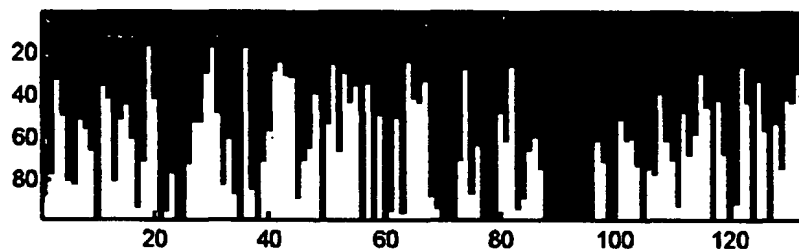
Figure 8: Result of signal-based classification in different color. PATD's are classified using the maximum-likelihood rule based on the PMF's in Fig. 6. The colorbar at the top indicates correct classification. Black dot appears when the PATD is equally likely to be classified to two or more classes.

11

Comparison of Different Temporal Measurements (Trial-based, full data)

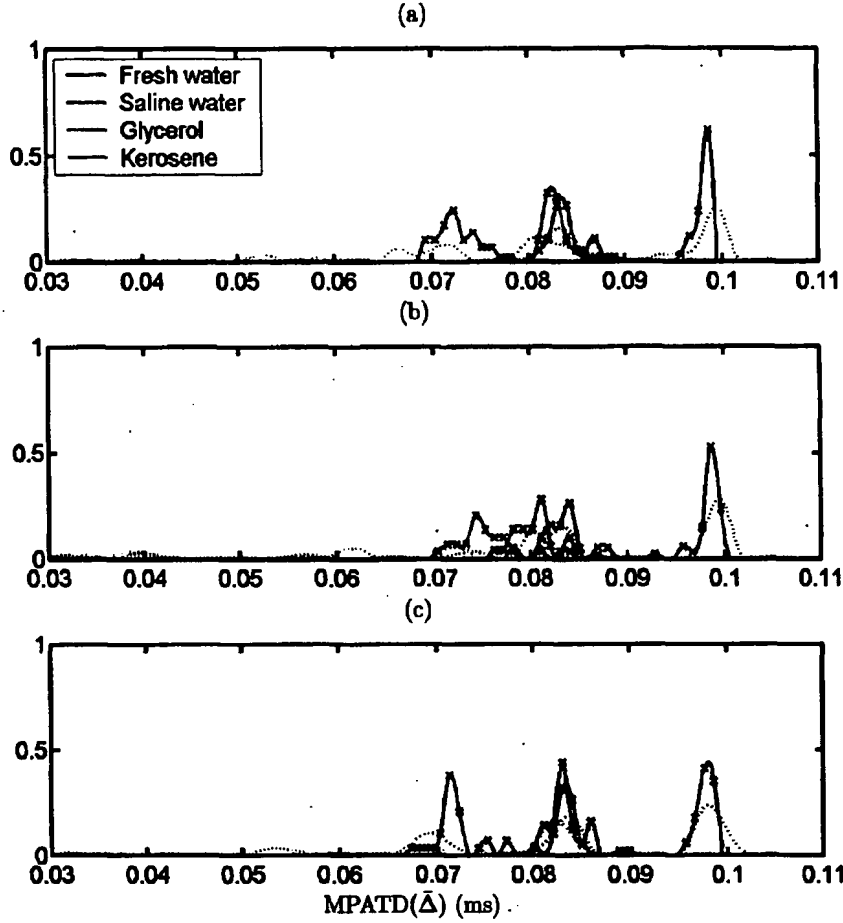(a)

(b)

(c)

MPATD($\bar{\Delta}$) (ms)

Figure 9: Dolphins emit several pinging signals for a single identification trial. Based on the measurements, we can see that the range of correct PATD is [0.065 ms, 0.107 ms]. (See Fig. 6.) In order to remove erroneous measurements, PATD values outside of this range can be safely removed. The mean peak arrival time difference (MPATD) of a trial is the mean value of PATD's within this range. The probability mass functions (PMFs) of MPATD's calculated from signals preprocessed in three different ways. The same color indication was used as in Fig. 6. Distributions of PATD are overlaid in dotted lines for comparison. Scale of PATD curve is adjusted according to the bin size change. (a) Absolute value. (b) Matched filtering. (c) Instantaneous envelope detection.

12

Comparison of Different Temporal Measurements (Trial-based, excluding outliers)

(a)

(b)
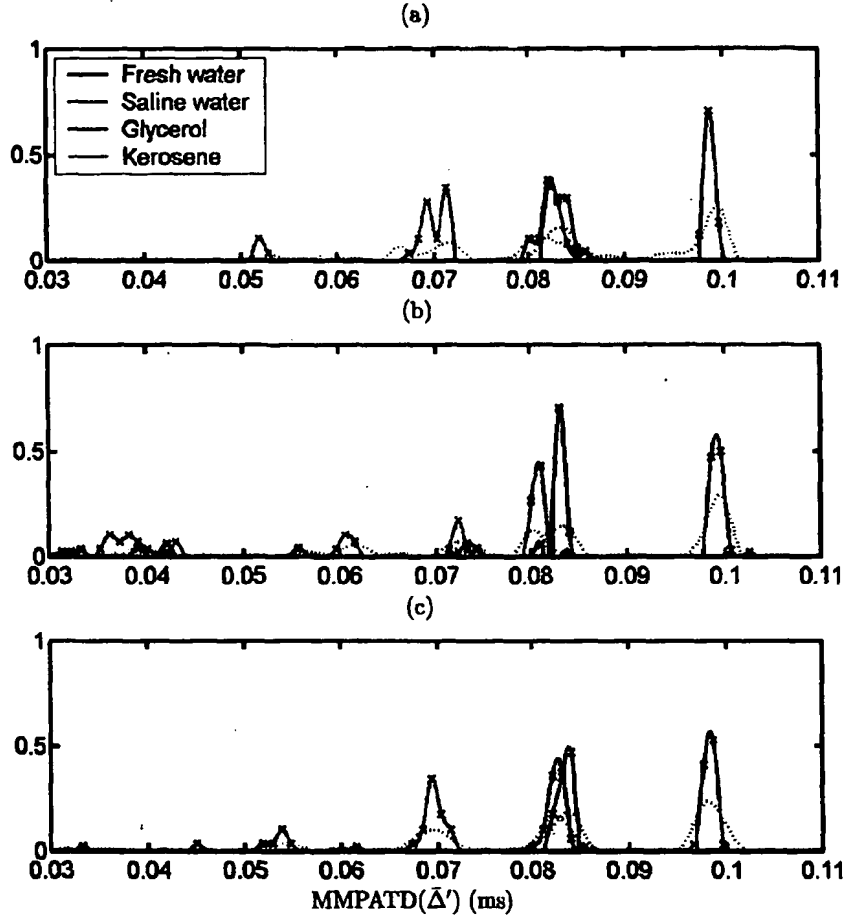
(c)

MMPATD($\bar{\Delta}'$) (ms)

Figure 10: Dolphins emit several pinging signals for a single identification trial. For the stability of classification, PATD's off from the center of the distribution of PATD in a trial are eliminated. The modified mean peak arrival time difference (MMPATD) of a trial is the mean value of those selected PATD's in the trial. The probability mass functions (PMFs) of MMPATD's calculated from signals preprocessed in three different ways. The same color indication was used as in Fig. 6. Distributions of PATD are overlaid in dotted lines for comparison. Scale of PATD curve is adjusted according to the bin size change. (a) Absolute value. (b) Matched filtering. (c) Instantaneous envelope detection.

13

Result of the Trial-Based Classification (MMPATD)

(a)

(b)

(c)

Trials

Figure 11: Result of trial-based classification in different color. MMPATD's are classified using the k-nearest neighbor method with $k = 5$. Black column appears when the trial is equally likely to be classified to two or more classes, or when MMPATD is not defined due to lack of data.

14

3.3 Combination of $\bar{\Delta}_m$ and $\bar{\Delta}_e$ for Fresh and Saline Water Separation

Trial-based classification of MMPATD has performed good separations of kerosene and glycerol trials from fresh and saline water trials when absolute value operated (Fig. 10(a)) or instantaneous envelope detection performed (Fig. 10(c)), but they didn't separate fresh and saline water trials from each other. In the mean time, the MMPATD's preprocessed by the matched filter have shown separable distributions, but the classification performance of those two classes was not satisfactory, because many of MMPATD's of fresh and saline water signals are mistaken by nearby MMPATD's of glycerol and kerosene MMPATD's during the k-nearest neighbor method. (Fig. 10(b).)

Hence, we are roused to combine two MMPATD's—one to determine whether the signal is from either of fresh or saline water, and the other one to separate fresh and saline water trials. We have tried two possible combinations of preprocessing methods—absolute value operation for water/non-water classes separation, matched filtering for fresh/saline separation, and envelope detection for water/non-water classes separation, matched filtering for fresh/saline separation. The results of each are presented in Table 3(a) and (b), and in Fig. 12(a) and (b).

	Fre	Sal	Gly	Ker	Total
$\Delta'_a \oplus \Delta'_m$	80.0%	98.0%	100.0%	100.0%	96.2%
$\bar{\Delta}'_e \oplus \bar{\Delta}'_m$	80.0%	94.0%	100.0%	100.0%	94.7%

Table 3: Performance of combined methods. $\bar{\Delta}'_a \oplus \bar{\Delta}'_m$ represents when $\bar{\Delta}'_a$ is used for the separation of fresh or saline water, glycerol, and kerosene classes, and $\bar{\Delta}'_m$ is used to separate fresh and saline water, etc.

4 Conclusion

Dolphins' returning signals are classified by different preprocessing and classification methods.

For the signal-based classification, the instantaneous envelope detection has produced most discriminating peak arrival time difference (PATD) between fresh or saline water, glycerol, and kerosene. In order to improve the discernibility, we have averaged PATD after screening by the fixed range (MPATD; by the acceptance range) and the variable range (MMPATD; by the mode cluster range). MPATD did not concentrate the probability distribution, while MMPATD has shown clear enhancement of separation between fresh or saline water, glycerol, and kerosene. Especially, matched filter treated MMPATD has shown the best separation between fresh and saline water classes, yielding up to 96.2 % of classification performance when two MMPATD classification methods are combined.

References

[1] R. L. Brill, M. L. Sevenich, J. Sullivan, J.D. Justman, and R. E. Witt. Behavioral evidence for hearing through the lower jaw by an echolocating dolphin (*Tursiops truncatus*). *Marine Mammal Science*, 4:223–230, 1988.

[2] H. C. Hughes. *Sensory Exotica*. MIT Press, Boston, 1999.

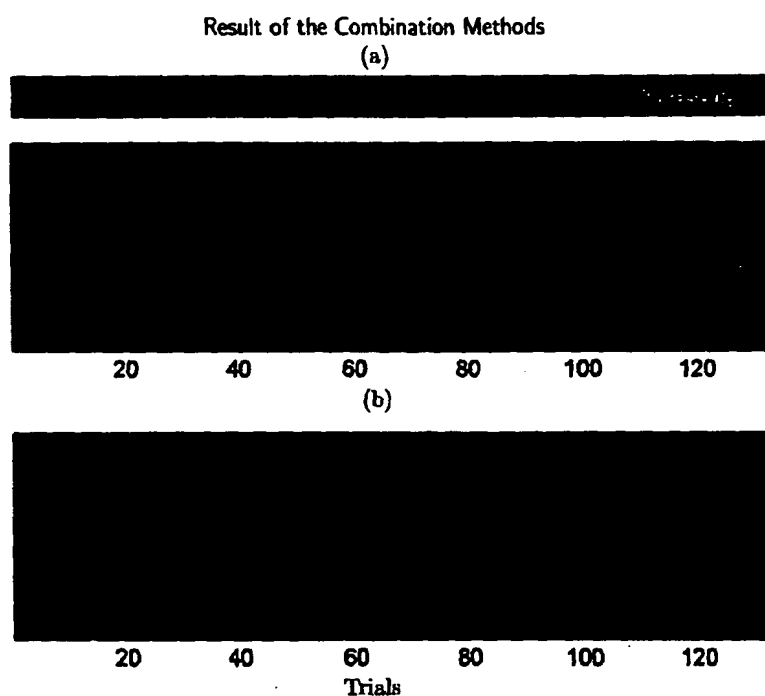**Result of the Combination Methods**

(a)

(b)

Figure 12: Result of combination method classification. Glycerol and kerosene classes are separated from water classes with use of $\bar{\Delta}'_a$ or $\bar{\Delta}'_e$, and then fresh and saline water classes are separated from each other by $\bar{\Delta}'_m$. (a) Classification by $\bar{\Delta}'_a \oplus \bar{\Delta}'_m$. (b) Classification by $\bar{\Delta}'_e \oplus \bar{\Delta}'_m$.

[3] H. L. Roitblat, Penner R. H., and Nachtigall P. E. Matching-to-sample by an echolocating dolphin. *Journal of Experimental Psychology: Animal behavior Processes*, 16:85–95, 1990.

[4] P. W. B. Moore, H. L. Roitblat, R. H. Penner, and P. E. Nachtigall. Recognizing successive dolphin echoes with an integrator gateway network. *Neural Networks*, 4:701–709, 1991.

[5] H. L. Roitblat, P. W. B. Moore, A. H. David, and P. E. Nachtigall. Representation and processing of acoustic information in a biomimetic neural network. In J.-A. Meyer, H. L. Roitblat, and S. W. Wilson, editors, *Animals to Animats 2: Simulation of Adaptive Behavior*, Boston, 1993. MIT Press.

[6] G. C. Gaunaurd, Brill D., and Huang H. Signal processing of the echo signatures returned by submerged shells insonified by dolphin clicks: Active classification. *Journal of the Acoustical Society of America*, 103:1547–1557, 1998.

[7] W. W. L. Au, J. L. Pawloski, P. E. Nachtigall, M. Bonz, and R. C Gisiner. Echolocation signals and transmission beam pattern of a false killer whale (*Pseudorca crassidens*). *Journal of the Acoustical Society of America*, 98:51–59, 1995.

[8] M. Kremliovsky, J. Kadtke, M. Inchiosa, and P. W. Moore. Characterization of dolphin acoustic echo-location data using a dynamical classification method. *International Journal of Bifurcation and Chaos*, 8(4):813–823, 1998.

[9] Merrill I. Skolnik. *Introduction to Radar Systems*. McGraw-Hill, London, third edition, 2001.

[10] Wolfgang Hess. *Pitch Determination of Speech Signals*. Springer-Verlag, Berlin, 1983.

[11] Rodger E. Ziemer, William H. Tranter, and Fannin D. Ronald. *Signals and Systems: Continuous and Discrete*. Macmillan Publishing Company, New York, 1993.

Document made available under the Patent Cooperation Treaty (PCT)

International application number: PCT/US04/025373

International filing date: 05 August 2004 (05.08.2004)

Document type: Certified copy of priority document

Document details: Country/Office: US
Number: 60/494,358
Filing date: 12 August 2003 (12.08.2003)

Date of receipt at the International Bureau: 06 December 2004 (06.12.2004)

Remark: Priority document submitted or transmitted to the International Bureau in compliance with Rule 17.1(a) or (b)